KINEMATIC ANALYSIS OF A STEWART PLATFORM BASED ON AFSA

Yuanhui TANG[1,3,*], Yiqi ZHUANG[2], Leping SHI[3], Yongguo JIA[4]

The direct kinematic problems (DKP) are of great importance for the design, use and control of Stewart platforms. It is proved that finding the solutions to DKP is still a basic and challenging problem. In this paper, the kinematics of a 6-6 Stewart platform has been investigated. The inverse and direct kinematic models have been developed. By employing the artificial fish swarm algorithm (AFSA), the solutions to the DKP are found. The results indicate that AFSA is an effective tool for solving DKPs of Stewart platforms. AFSA can be extended to solve other parallel mechanisms' DKPs.

Keywords: Stewart platform; Artificial fish swarm algorithm; Direct kinematic problems

List of symbols
$^{O}\boldsymbol{a}_i$: Coordinates of nodes A_i in the fixed reference frame $O(X, Y, Z)$
$^{O}\boldsymbol{b}_i$: Coordinates of nodes B_i in the fixed reference frame $O(X, Y, Z)$
$^{O'}\boldsymbol{b}_i$: Coordinates of nodes B_i in the fixed reference frame $O'(X', Y', Z')$
R: The radius of the circumcircle of the base hexagon of the Stewart platform
r: The radius of the circumcircle of the mobile hexagon of the Stewart platform
$\boldsymbol{T}$: The rotation matrix
S_t: Step length of AFSA.
N: The number of artificial fishes.
V: Visual distance of AFSA.
L_i: Length of A_iB_i

1. Introduction

The Stewart platform has the advantages of high load carrying capacity, good dynamic performance, better accuracy, higher rigidity, higher load to weight ratio and precise positioning capability. Due to these attractive characteristics, the Stewart platform has been used in many disciplines, such as flight simulators [1], vibration isolation system [2], mounting of telescopic equipment [3], etc.

[1] School of Electro-Mechanical Engineering, Xidian University, CHINA.
[2] School of Microelectronics, Xidian University, CHINA.
[3] Shaanxi Institute of Metrology Science, CHINA.
[4] Shaanxi Institute of Metrology Science, CHINA.
[*] Corresponding author: Yuanhui Tang, Email: 7985945@qq.com

In the past decades, Stewart platforms have received great attention from many researchers. Considerable research works have been carried out on dynamics and motion control of Stewart platforms. Wang et al. [4] investigated the active vibration isolation of a Stewart platform manipulator with piezoelectric actuators. Geng [5] proposed an active vibration isolation system with Stewart form and adopted robust adaptive filter algorithms for active vibration control. Based on the principle of virtual work, Staicu [6] studied the dynamics of a 6-6 Stewart parallel manipulator. Huang and Fu [7] researched motion control of Stewart platforms based on a sliding-mode control technique. Although the control of the Stewart platform has been investigated by many researchers, the control problem calls for the solution of the direct kinematics, which is still a basic and challenging problem as well.

The direct kinematic problems, which is to determine the positions and orientations of the moving platform given the lengths of the six legs, lead naturally to system of nonlinear algebraic and transcendental equations. Many scholars research the closed-form solutions for different types and geometry. Griffis [8] and Inocenti [9] obtained a 16th degree univariate polynomial on the general 3-6 Stewart platform. Innocenti [10] obtained all 32 solutions to the forward kinematics of the type 4-6. However, devising a common algorithm to find the solutions to the direct kinematic problem of any types of Stewart has proved to be a challenging undertaking. Moreover, finding the solutions to the direct kinematic problems by numerical techniques is quite practical in real time controlling process. McAree [12] implemented impressive Newton-Raphson scheme to obtain fast and reliable direct kinematic solution. Geng and Haynes [13] and Yee and Lim [14] implemented the network on the direct kinematic problem. By using Newton iterative method, a solution to any type of Stewart platform can be found. However, the Newton iterative method has a shortcoming that it is sensitive to the initial values. Recently, immune genetic algorithm is employed to solve the direct kinematics of the Stewart platform [11], which can be considered as an effective tool in solving the direct kinematic problems. In this paper, artificial fish swarm algorithm (AFSA) is used to find the solutions to the direct kinematic problem of a 6-6 Stewart platform, which has the potential to obtain near-global minimum. AFSA has been successfully applied to many complicated optimization problems.

This paper is organized as follows. First, the architecture of the 6-6 Stewart platform is presented in section 2. Secondly, the kinematics of the Stewart platform is discussed in detail in section 3. Third, AFSA is described in section 4. The numerical example is simulated in section 5. Finally, conclusion and the future work are reported in section 6.

2. Mechanism description

A diagram of the Stewart platform is shown in Fig. 1. It consists of two platforms and six legs. The base platform denoted by nodes A_1, A_2, A_3, A_4, A_5 and A_6 is fixed to the ground. The mobile platform denoted by nodes B_1, B_2, B_3, B_4, B_5 and B_6 can generate translational and rotational movements. Moreover, the legs A_iB_i (i = 1, 2, 3, 4, 5, 6) are prismatic actuators that are used to vary the distances between nodes A_i and B_i. From Figure 1, it can be shown that the mobile and base platforms are both regular hexagons. The radius of the circumcircle of the base hexagon is R while the radius of the circumcircle of the mobile hexagon is r. Furthermore, the legs A_iB_i of length L_i are jointing to the mobile and base platforms by spherical joints.

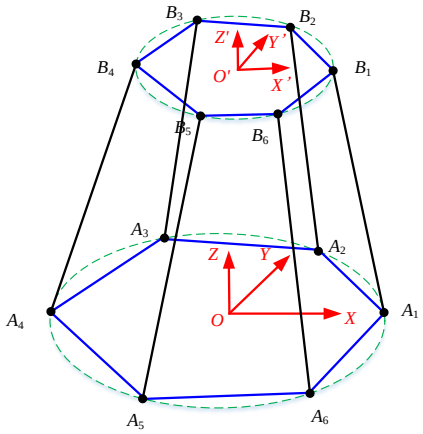

Figure 1 Stewart platform

As illustrated in Figure 1, a fixed reference frame O (X, Y, Z) is located at the center of the base hexagon while a moving reference frame O' (X ', Y ', Z ') is located at the center of the mobile hexagon. The X axis of the fixed reference frame is parallel to the line joining nodes O and A_1 while its Z axis is perpendicular to the base hexagon. In the meantime, the X' axis of the moving reference frame is parallel to the line joining nodes O' and B_1 while the Z' axis is perpendicular to the mobile hexagon. Since the legs are connecting to the fixed and mobile platforms by spherical joints, the mobile platform can generate translations along X, Y and Z axis respectively and rotations around X, Y and Z axis respectively. For this reason, it is appropriate to say that the mechanism has six degrees of freedom. The coordinates of the point O' are defined as x, y and z. The position and orientation of the mobile platform can be described by the position vector $\boldsymbol{P} = [x, y, z]^T$ and the rotation matrix $\boldsymbol{T}$ with respect to the fixed reference frame. Here the rotation matrix $\boldsymbol{T}$ is defined by rotating the moving reference frame α about Z' axis and followed β about Y' axis, γ about Z' axis. As a consequence, $\boldsymbol{T}$ takes the following form

$$\boldsymbol{T}=\begin{bmatrix}\cos\alpha\cos\beta & \cos\alpha\sin\beta\sin\gamma-\sin\alpha\cos\gamma & \cos\alpha\sin\beta\cos\gamma+\sin\alpha\sin\gamma\\ \sin\alpha\cos\beta & \sin\alpha\sin\beta\sin\gamma-\cos\alpha\cos\gamma & \sin\alpha\sin\beta\sin\gamma-\cos\alpha\sin\gamma\\ -\sin\beta & \cos\beta\sin\gamma & \cos\beta\cos\gamma\end{bmatrix} \quad (1)$$

From Fig. 1, it can be seen that the shape of the Stewart platform can be controlled by varying the legs' lengths L_i. Therefore, the lengths L_i are chosen as the Stewart platform's input variables while the movements of the mobile hexagon expressed by variables x, y, z, α, β and γ are chosen as the Stewart platform's output. The relations between the input and output variables are of great importance when such a mechanism is put to use. In the following sections, the kinematic analysis of the Stewart platform will be discussed.

3. Kinematic analysis

3.1 Inverse kinematic problem

The inverse kinematic problem of the Stewart platform corresponding to the computation of the legs' lengths for given the position and orientation of the mobile hexagon. For the Stewart platform studied here, the vectors specifying the positions of nodes A_i and B_i in the fixed reference frame are defined as ${}^{O}\boldsymbol{a}_i$ and ${}^{O}\boldsymbol{b}_i$, respectively. Also, the vectors specifying the positions of nodes B_i in the moving reference frame are defined as ${}^{O'}\boldsymbol{b}_i$. From Figure 1, the vectors specifying the positions of nodes A_i in the fixed reference frame can be easily derived.

$${}^{O}\boldsymbol{a}_1=\begin{bmatrix}R\\0\\0\end{bmatrix},{}^{O}\boldsymbol{a}_2=\begin{bmatrix}\frac{R}{2}\\\frac{\sqrt{3}}{2}R\\0\end{bmatrix},{}^{O}\boldsymbol{a}_3=\begin{bmatrix}-\frac{R}{2}\\\frac{\sqrt{3}}{2}R\\0\end{bmatrix},{}^{O}\boldsymbol{a}_4=\begin{bmatrix}-R\\0\\0\end{bmatrix},{}^{O}\boldsymbol{a}_5=\begin{bmatrix}-\frac{R}{2}\\-\frac{\sqrt{3}}{2}R\\0\end{bmatrix},{}^{O}\boldsymbol{a}_6=\begin{bmatrix}\frac{R}{2}\\-\frac{\sqrt{3}}{2}R\\0\end{bmatrix} \quad (2)$$

Similarly, the vectors specifying the positions of nodes B_i in the moving reference frame can be easily computed.

$${}^{O'}\boldsymbol{b}_1=\begin{bmatrix}r\\0\\0\end{bmatrix},{}^{O'}\boldsymbol{b}_2=\begin{bmatrix}\frac{b}{2}\\\frac{\sqrt{3}}{2}b\\0\end{bmatrix},{}^{O'}\boldsymbol{b}_3=\begin{bmatrix}-\frac{r}{2}\\\frac{\sqrt{3}}{2}r\\0\end{bmatrix},{}^{O'}\boldsymbol{b}_4=\begin{bmatrix}-r\\0\\0\end{bmatrix},{}^{O'}\boldsymbol{b}_5=\begin{bmatrix}-\frac{r}{2}\\-\frac{\sqrt{3}}{2}r\\0\end{bmatrix},{}^{O'}\boldsymbol{b}_6=\begin{bmatrix}\frac{r}{2}\\-\frac{\sqrt{3}}{2}r\\0\end{bmatrix} \quad (3)$$

Considering the position vector $\boldsymbol{P} = [x, y, z]^T$ and the rotation matrix $\boldsymbol{T}$, the position vectors of points B_i (i = 1, 2, 3, 4) with respect to the fixed reference frame can be obtained:

$$ {}^{O}\boldsymbol{b}_i = \boldsymbol{P} + \boldsymbol{T} \cdot {}^{O'}\boldsymbol{b}_i,\ i = 1,\ 2,\ 3,\ 4,\ 5,\ 6 \tag{4} $$

With the position vectors of points A_i and B_i now known, the vector of the ith leg can be written as

$$ \boldsymbol{L}_i = {}^{O}\boldsymbol{b}_i - {}^{O}\boldsymbol{a}_i,\ i = 1,\ 2,\ 3,\ 4,\ 5,\ 6 \tag{5} $$

Therefore, the length of the ith leg can be given as

$$ L_i = \left| {}^{O}\boldsymbol{b}_i - {}^{O}\boldsymbol{a}_i \right|,\ i = 1,\ 2,\ 3,\ 4,\ 5,\ 6 \tag{6} $$

By substituting Eqs. (2) and (4) into Eq. (6), the solutions to the inverse kinematic problem can be obtained.

$$ \begin{aligned} Eq_1 = {} & \left[x - R - r(\sin\alpha\sin\gamma - \cos\alpha\cos\beta\cos\gamma)\right]^2 + \\ & \left[y + r(\cos\alpha\cos\gamma + \sin\alpha\cos\beta\cos\gamma)\right]^2 + (z - r\sin\beta\cos\gamma)^2 = L_1^2 \end{aligned} \tag{7} $$

$$ \begin{aligned} Eq_2 = {} & \left[x - 0.5R + r\cos\alpha\cos\beta\cos\left(\frac{\pi}{3} + \gamma\right) - r\sin\alpha\sin\left(\frac{\pi}{3} + \gamma\right)\right]^2 + \\ & \left[y - \frac{\sqrt{3}}{2}R + r\cos\alpha\sin\left(\frac{\pi}{3} + \gamma\right) + r\sin\alpha\cos\beta\cos\left(\frac{\pi}{3} + \gamma\right)\right]^2 + \\ & \left[z - r\sin\beta\cos\left(\frac{\pi}{3} + \gamma\right)\right]^2 = L_2^2 \end{aligned} \tag{8} $$

$$ \begin{aligned} Eq_3 = {} & \left[x + 0.5R + r\sin\alpha\sin\left(\gamma - \frac{\pi}{3}\right) - r\cos\alpha\cos\beta\cos\left(\gamma - \frac{\pi}{3}\right)\right]^2 + \\ & \left[y - \frac{\sqrt{3}}{2}R - r\cos\alpha\sin\left(\gamma - \frac{\pi}{3}\right) - r\sin\alpha\cos\beta\cos\left(\gamma - \frac{\pi}{3}\right)\right]^2 + \\ & \left[z + r\sin\beta\cos\left(\gamma - \frac{\pi}{3}\right)\right]^2 = L_3^2 \end{aligned} \tag{9} $$

$$ \begin{aligned} Eq_4 = {} & \left[x + R + r\left(\sin\alpha\sin\gamma - \cos\alpha\cos\beta\cos\gamma\right)\right]^2 + \\ & \left[y - r(\cos\alpha\sin\gamma + \sin\alpha\cos\beta\cos\gamma)\right]^2 + \left[z + r\cos\gamma\sin\beta\right]^2 = L_4^2 \end{aligned} \tag{10} $$

$$Eq_5 = \left[x + \frac{R}{2} + r\sin\alpha\sin\left(\gamma + \frac{\pi}{3}\right) - r\cos\alpha\cos\beta\cos\left(\gamma + \frac{\pi}{3}\right)\right]^2 +$$
$$\left[y + \frac{\sqrt{3}R}{2} - r\cos\alpha\sin\left(\gamma + \frac{\pi}{3}\right) - r\sin\alpha\cos\beta\cos\left(\gamma + \frac{\pi}{3}\right)\right]^2 + \quad (11)$$
$$\left[z + r\sin\beta\cos\left(\gamma + \frac{\pi}{3}\right)\right]^2 = L_5^2$$

$$Eq_6 = \left[x - \frac{R}{2} - r\sin\alpha\sin\left(\gamma - \frac{\pi}{3}\right) - r\cos\alpha\cos\beta\cos\left(\gamma - \frac{\pi}{3}\right)\right]^2 +$$
$$\left[y + \frac{\sqrt{3}R}{2} + r\cos\alpha\sin\left(\gamma - \frac{\pi}{3}\right) + r\sin\alpha\cos\beta\cos\left(\gamma - \frac{\pi}{3}\right)\right]^2 + \quad (12)$$
$$\left[z - r\sin\beta\cos\left(\gamma - \frac{\pi}{3}\right)\right]^2 = L_6^2$$

With the given input variables x, y, z, α, β and γ, the legs' lengths L_i (i = 1, 2, 3, 4, 5, 6) can be easily computed by using Eqs. (7)-(12).

3.2 Direct kinematic problem

Direct kinematic problem consists in computing the position and rotation variables for the legs' lengths.

When the input variables L_i are given, the solutions to the direct kinematic problem can be obtained by combining Eqs. (7)-(12). Generally, the analytical solutions to Eqs. (7)-(12) do not exist. During the past half-century, considerable research has been performed on finding numerical solutions to the direct kinematic problem. However, less well-validated methods are found to solve the direct kinematic problems of all kinds of Stewart platforms. With the development of intelligent optimization algorithm, artificial fish swarm algorithm are employed in this work to solve the direct kinematic problem to the Stewart platform.

4. Artificial fish swarm algorithm

The Artificial fish swarm algorithm (AFSA) is an intelligent optimization algorithm proposed by Li [15] inspired by the social behaviors of fish swarm in search of food. The fish swarm behaviors include praying behavior, leaping behavior, swarming behavior and swallowing behavior. The AFSA is mainly used to solve optimization problems. It works with a group of artificial fishes referred

to as a swarm. Each individual called an artificial fish (AF) denotes a feasible solution to the optimization problem. By evaluating AF's behaviors, each AF moves a step in the search space towards the better AF. After a number of iteration times, AFs will be around the better solutions to the optimization problem. The AFSA can search the global optimum effectively and adaptively.

4.1 Optimization model

In order to solve the direct kinematic problem of the Stewart platform, an optimization model will be developed firstly. Eqs. (7)-(12) can be rewritten as

$$Eq_k - L_k^2 = 0,\ (k = 1,\ 2,\ 3,\ 4,\ 5,\ 6) \tag{13}$$

The equivalence model is constructed of Eq. (13) as

$$\begin{aligned} &\text{minimize} && f(x, y, z, \alpha, \beta, \gamma) = \sum_{k=1}^{6} \left(Eq_k - L_k^2 \right)^2 \\ &\text{subject to} && x_{\min} \le x \le x_{\max},\ y_{\min} \le y \le y_{\max}, z_{\min} \le z \le z_{\max} \\ & && \alpha_{\min} \le \alpha \le \alpha_{\max}, \beta_{\min} \le \beta \le \beta_{\max}, \gamma_{\min} \le \gamma \le \gamma_{\max} \end{aligned} \tag{14}$$

From Eq. (14), it can be seen that the minimum of $f(x, y, z, \alpha, \beta, \gamma)$ is zero. According to the AFSA, each AF denotes a feasible solution to the optimization problem expressed by Eq. (14). The best AF will satisfy $f(x, y, z, \alpha, \beta, \gamma) = 0$. Moreover, when the best AF is found, the corresponding values of x, y, z, α, β and γ will be the solutions to the direct kinematic problem described by Eqs. (7)-(12).

4.2 Behaviors of Artificial fish

Let N be the number of AFs. The AF_i ($i \in \{1, 2, \ldots, N\}$) is associated with a vector $\boldsymbol{X}_i = [x^i, y^i, z^i, \alpha^i, \beta^i, \gamma^i]^T$ while the food consistence of the AF_i is associated with $Y_i = f(\boldsymbol{X}_i)$. The realization of the behaviors in AFSA is as follows.

1) Praying behavior

It is assumed that the current position of an AF is denoted by $\boldsymbol{X}_i^t$. Before the praying behavior occurs, the AF will select a state $\boldsymbol{X}_j$ randomly within its visual distance firstly.

$$\boldsymbol{X}_j = \boldsymbol{X}_i^t + V \cdot Rand() \tag{15}$$

Where $Rand()$ is a random number within the interval [0, 1] and V is the visual distance of the AF. For the minimum problem expressed by Eq. (14), if $Y_j < Y_i$, the AF will go a step towards Y_j. Let $\boldsymbol{X}_i^{t+1}$ be the AF's next position, it takes the following form

$$\boldsymbol{X}_i^{t+1} = \boldsymbol{X}_i^t + \frac{\boldsymbol{X}_j - \boldsymbol{X}_i^t}{\left\| \boldsymbol{X}_j - \boldsymbol{X}_i^t \right\|} \cdot S_t \cdot Rand() \tag{16}$$

Where S_t is the AF's moving step length. However, it $Y_j > Y_i$, the AF will select another state $\boldsymbol{X}_j$ randomly again and judge whether it satisfies the forward requirement. Moreover, if the forward requirement cannot be satisfied after several times denoted by T_r, the AF will move step randomly.

$$\boldsymbol{X}_i^{t+1} = \boldsymbol{X}_i^t + V \cdot Rand() \tag{17}$$

2) Swarming behavior

Let $\underline{n_f}$ be the numbers of the AF's companions within its visual range. The center position of the AFs including the AF itself and its companions is denoted by $\boldsymbol{X}_c$. If $Y_c/n_f < \delta Y_i$, which means that more fitness values exist around the center $\boldsymbol{X}_c$ and the surrounding environment is not very crowded, the AF will go a step towards the center $\boldsymbol{X}_c$ from its current position $\boldsymbol{X}_i$.

$$\boldsymbol{X}_i^{t+1} = \boldsymbol{X}_i^t + \frac{\boldsymbol{X}_c - \boldsymbol{X}_i^t}{\left\| \boldsymbol{X}_c - \boldsymbol{X}_i^t \right\|} \cdot S_t \cdot Rand() \tag{18}$$

Otherwise, the AF will choose the preying behavior.

3) Following behavior

Let $\boldsymbol{X}_i$ be the AF's current state. It explores its neighborhood area to find the companion $\boldsymbol{X}_j$ which has the best food consistence. If $\boldsymbol{Y}_j/n_f < \delta Y_i$, which means that the AF $\boldsymbol{X}_j$ has lower fitness value and the surrounding environment is not very crowed, the AF $\boldsymbol{X}_i$ will go a step towards $\boldsymbol{X}_j$.

$$\boldsymbol{X}_i^{t+1} = \boldsymbol{X}_i^t + \frac{\boldsymbol{X}_c - \boldsymbol{X}_i^t}{\left\| \boldsymbol{X}_c - \boldsymbol{X}_i^t \right\|} \cdot S_t \cdot Rand() \tag{19}$$

4) Moving behavior

The Moving behavior of an AF corresponds to the situation that the AF moves randomly within its visual range, which is given by

$$\boldsymbol{X}_i^{t+1} = \boldsymbol{X}_i^t + V \cdot Rand() \tag{20}$$

4.3 The procedure of AFSA

The procedure of AFSA is given as follows

Step1. Initialize the parameters of the AFSA including the number of AFs N, the current state of each AF $\boldsymbol{X}_i$, AF's step length S_t, AF's visual distance V, try numbers T_r and crowding factor δ.

Step2. Compute the food consistence of each AF and record the state of the best AF.

Step3. Evaluate the states of each AF and choose the behaviors of each AF to be executed.

Step4. Execute each AF's behavior and update its location information.

Step5. Update the state of the best AF.

Step6. Stop and display the result if the stop condition is satisfied, otherwise, return to step 2.

5 Numerical simulations

For the Stewart platform shown in Fig. 1, the given input variables are selected as L_1 = 2.0 m, L_2 = 1.8 m, L_3 = 2.3 m, L_4 = 2.8 m, L_5 = 2.8 m and L_6 = 2.5m. Moreover, the parameters of the fixed and mobile hexagons are set to be R = 2 m and r = 1 m. Solving the optimization model described by Eq. (14), the output variables x, y, z, α, β and γ can be obtained. The coefficients of Eq. (14) and the parameters of AFSA are listed in Table 1.

Table 1

Coefficients of the optimization and parameters of AFSA

Coefficient	Value	Unit
$x_{\min}$	-4	m
$x_{\max}$	4	m
$y_{\min}$	-4	m
$y_{\max}$	4	m
$z_{\min}$	0	m
$z_{\max}$	4	m
$\alpha_{\min}$	-π/2	--
$\alpha_{\max}$	π/2	--
$\beta_{\min}$	-π/2	--
$\beta_{\max}$	π/2	--
$\gamma_{\min}$	-π/2	--
$\gamma_{\max}$	π/2	--
T_r	5	--
S_t	0.2	--
V	6	--
N	20	--

Let $\boldsymbol{X}_{\text{best}}$ be the best AF for each iteration. Solving Eq. (14) by AFSA, the obtained food consistence of $\boldsymbol{X}_{\text{best}}$ is shown in Figure 2.

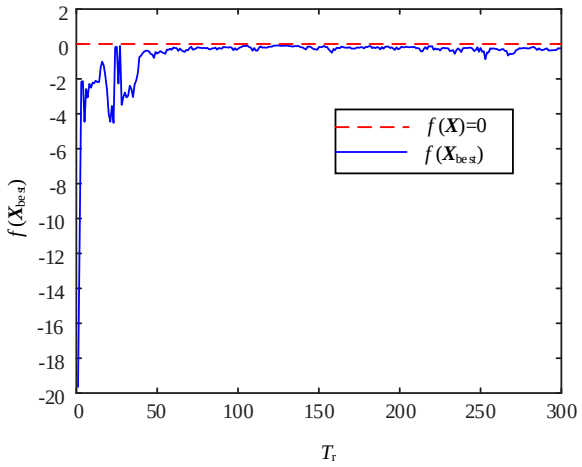

Fig. 2 Food consistence of $\boldsymbol{X}_{\text{best}}$

In Fig. 2, T_r denotes the iterate times. From Fig. 2, it can be seen that after 50 iterations, the consistence of $\boldsymbol{X}_{\text{best}}$ approximates to zero. This means that the obtained $\boldsymbol{X}_{\text{best}}$ by AFSA approaches the true solution to Eq. (14). Then, $\boldsymbol{X}_{\text{best}}$ can be considered as the solution to the direct kinematic problem. After 300 iterations, the obtained $\boldsymbol{X}_{\text{best}}$ is $\boldsymbol{X}_{\text{best}} = [x_{\text{best}}, y_{\text{best}}, z_{\text{best}}, \alpha_{\text{best}}, \beta_{\text{best}}, \gamma_{\text{best}}]^T = [0.5, 0.5, 1.5, 0.52, 0.53, 0.52]^T$.

Since the minimum of $f(\boldsymbol{X})$ is zero, the error of AFSA is defined as the difference between $f(\boldsymbol{X}_{\text{best}})$ and zero, which is given by

$$\varepsilon = \left| f(\boldsymbol{X})_{\min} - f(\boldsymbol{X}_{\text{best}}) \right| = \left| f(\boldsymbol{X}_{\text{best}}) \right| \tag{21}$$

Keeping the number of AFs N and the visual distance V constant (N = 20 and V = 6), the variation of the error ε with the step length S_t is shown in Figure 3. Keeping St and N constant (S_t = 0.1 and N = 20), the variation of the error ε with the visual distance V is shown in Fig. 4. Moreover, Fig. 5 shows variation of the error ε with number of AFs with S_t = 0.1 and V = 6.

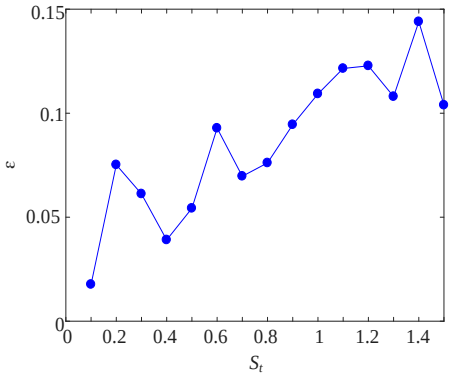

Fig. 3 Variation of ε with S_t

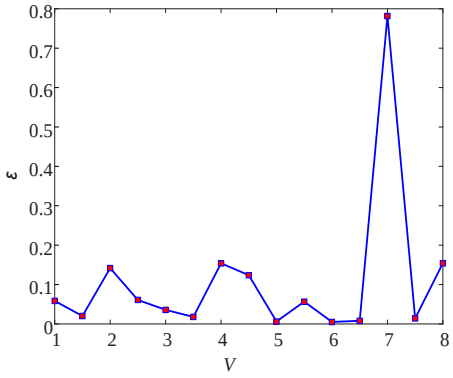

Fig. 4 Variation of ε with V

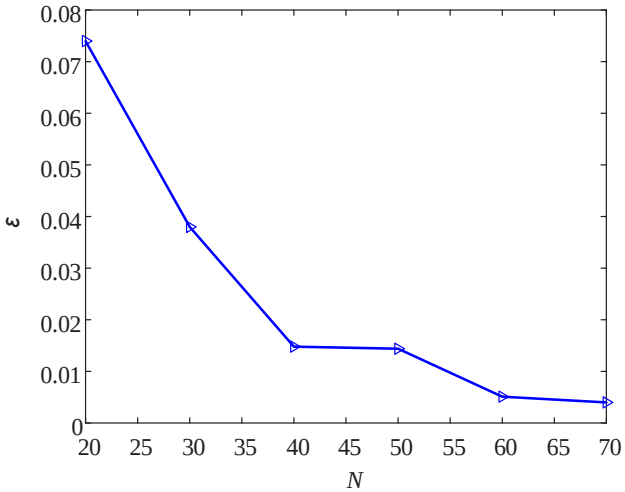

Fig. 5 Variation of ε with N

From Fig. 3, it can be seen that AFSA has better precision when the step length is 0.1. When this is the case, the difference between $f(\boldsymbol{X}_{\text{best}})$ and $f(\boldsymbol{X})_{\min}$ is 0.0177. From Fig. 4, it can be seen that AFSA has better precision when $V = 6$. In order to obtain a better solution to the direct kinematic problem, appropriate step length and visual distance should be chosen. Moreover, from Figure 5, it can be seen that the error ε decreases with an increase in the number of AFs. This means that the precision increases with N. However, if the number of AFs increases, the time needed for computation will be increased. When solving the direct kinematic problem by AFSA, less AFs should be chosen under meeting the condition of precision.

Furthermore, AFSA can also be used to detect the singularities of the Stewart platform. By differentiating Eqs. (7)-(12), the Jacobian, $\boldsymbol{J}$, relating a set of infinitesimal changes of the Stewart platform's input variables (δL) to the infinitesimal changes of its output variables (δX) can be obtained.

$$\delta \boldsymbol{L} = \boldsymbol{J} \cdot \delta \boldsymbol{X} \tag{22}$$

where

$$\begin{cases} \boldsymbol{X} = \begin{bmatrix} x & y & z & \alpha & \beta & \gamma \end{bmatrix}^T \\ L = \begin{bmatrix} L_1 & L_2 & L_3 & L_4 & L_5 & L_6 \end{bmatrix}^T \end{cases} \tag{23}$$

In Eq. (22), the elements $\boldsymbol{J}$ can be expressed by the output variables. The singular configurations of the Stewart platform correspond to situations where the determinant of $\boldsymbol{J}$ is zero, goes to infinity or is indeterminate. Since the output variables is obtained by AFSA for the given input variables. Afterwards, by substituting the output variables into Eq. (22) and computing the determinant of $\boldsymbol{J}$, the singular configurations of the Stewart platform can be detected.

6 Conclusion

A numerical approach for finding the solutions of a 6-6 Stewart platform has been researched based on AFSA. Firstly, the architecture of the Stewart platform is introduced. Then, the direct and inverse kinematic equations have been developed. Afterwards, by converting the direct kinematic problem into an optimization model, AFSA is employed to find the solutions to the direct kinematic problems. Finally, the numerical simulations have been completed. The results indicate that AFSA is an effective tool for solving the direct kinematics of a Stewart platform. Moreover, the appropriate coefficients of AFSA have been determined for the given geometric parameters of the Stewart platform. Generally, precision of AFSA increases with the number of AFs. Furthermore, the results confirmed that AFSA can be considered an alternative approach for the direct kinematic problems of the Stewart platform.

REFERENCES

[1]. *D. Stewart*, "A platform with six degrees of freedom", Proceedings of Institute of Mechanical Engineering, vol. 180, no. 1, 1965, pp. 371-386.

[2]. *A. Preumont, M. Horodinca, I. Romanescu, et al.*, "A six-axis single-stage active vibration isolator based on Stewart platform". Journal of Sound and Vibration, vol. 300, no. 3-5, 2007, pp. 644-661.

[3] *Y. Su and B. Duan*, "The application of the Stewart platform in large spherical radio telescopes", Journal of Robotic Systems, vol. 17, no. 7, 2000, pp. 375-83.

[4] *C. Wang, X. Xie, Y. Chen, et al*., "Investigation on active vibration of a Stewart platform with piezoelectric actuators", Journal of Sound and Vibration, vol. 383, 2016, pp. 1-19.

[5] *Z. J. Geng and L. S. Haynes*, "Six degree-of-freedom active vibration control using the Stewart platforms", IEEE Transactions on Control Systems Technology, vol. 2, no. 1, 1994, pp. 45-53.

[6]. *S. Staicu*, "Dynamics of the 6-6 Stewart parallel manipulator", Robotics and Computer-Intergrated Manufacturing, vol. 27, no. 1, 2011, pp. 212-220.

[7] *C. Huang and L. Fu*, "Adaptive backstepping tracking control of the Stewart platform", 43rd IEEE Conference on Decision and Control, vol. 5, 2004, pp. 5288-5233.

[8] *M. Griffis, J. Duffy*, "A forward displacement analysis of a class of Stewart platforms", Journal of Robotic Systems, vol. 6, no. 6, 1989, pp. 703-720.

[9] *C. Innocenti and V. Parenti-Catelli*, "Direct position analysis of the Stewart platform mechanism", Mechanism and Machine Theory, vol. 25, no. 6, 1990, pp. 611-621.

[10] *C. Innocenti*, "Direct kinematics in analytical form of the 6-4 fully parallel mechanism", Journal of Mechanical Design, vol. 117, no. 1, 1995, pp. 89-95.

[11] *S. Liu, W. Li, Y. Du, et al.*, "Forward kinematics of the Stewart platform using hybrid immune genetic algorithm", International Conference on Mechatronics and Automation. IEEE, 2006: 2330-2335.

[12] *P. R. McAree and R. W. Daniel*. "A fast, robust solution to the Stewart platform forward kinematics", Journal of Robotic Systems, vol. 13, no. 7, 1996, pp. 407-427.

[13] *G. Zheng and L. S. Haynes*, "Network solution for the forward kinematics problem of a Stewart platform", International Conference on Robotics and Automation. IEEE, 1991: 2650-2655.

[14] *S. Y. Choon and K. Lim*, "Forward kinematics solution of Stewart platform using neural networks", Neurocomputing, vol. 16, no. 4, 1997, pp. 333-349.

[15] *X. Li*. A new intelligent optimization-artificial fish swam algorithm. PhD thesis. Zhejiang University, China, 2003.